Materials and Methods

Worm strains, plasmids and ATFS-1 expression

The reporter strains *hsp-60$_{pr}$::gfp(zcIs9)V* and *atfs-1$_{pr}$::atfs-1::gfp* have been described previously (*3, 5*). Where indicated, the *hsp-60$_{pr}$::gfp(zcIs9)V* transgene was crossed into individual mutant strains of interest, with the exception of *atfs-1(tm4525)V*, which was backcrossed with the N2 strain three times prior to crossing into the *hsp-60$_{pr}$::gfp* background. The *clk-1(qm30)* and *isp-1(qm150)* strains were obtained from the Caenorhabditis Genetics Center (Minneapolis, MN). The *atfs-1(tm4525)* and *lon(tm5171)* (*C. elegans* gene name *c34b2.6*) strains were obtained from the National BioResource Project (Tokyo, Japan). RNAi feeding experiments were performed as described (*3*).

To generate the ATFS-1$^{1\text{-}100}$::GFP mammalian expression plasmid, a PCR product corresponding to the first 100 amino acids of *C. elegans* ATFS-1 was amplified from cDNA and cloned into the peGFP-N1 plasmid. The *C. elegans hsp-16$_{pr}$::atfs-1$^{\Delta 1\text{-}32.myc}$* expression plasmid was generated by PCR amplifying from N2 cDNA a fragment corresponding to amino acids 33-472 of ATFS-1 and cloning in frame and downstream of the Myc epitope sequences in the *hsp-16$_{pr}$::^{TAG}ubl-5* plasmid (*10*), replacing the *ubl-5* open reading frame. The *hsp-16$_{pr}$::atfs-1$^{\Delta 1\text{-}32.myc}$::gfp* expression plasmid was generated by ligating an *ApaI-SalI* fragment containing the 3` end of *atfs-1* and GFP from the *atfs-1$_{pr}$::atfs-1::gfp* expression plasmid (*5*) into similarly digested *hsp-16$_{pr}$::atfs-1$^{\Delta 1\text{-}32.myc}$*. The *hsp-16$_{pr}$::atfs-1^{FL}* expression plasmid was generated by PCR amplification of the *atfs-1* open reading frame from cDNA and ligating it into *NheI-EcoRV* digested *hsp-16$_{pr}$::atfs-1$^{\Delta 1\text{-}32.myc}$* which removes the Myc sequences placing the *atfs-1^{FL}* sequence downstream of the *hsp-16* promoter. The *hsp-16$_{pr}$::atfs-1$^{\Delta 1\text{-}32.myc.\Delta NLS}$* expression plasmid was generated by changing amino acids 433-444 from AAVRYREKKRAE to AAVAYREAARAE altering the predicted NLS (*16*). The *hsp-16$_{pr}$::ATFS-1$^{N\text{-}NLS}$* plasmid was generated by changing amino acids 84-96 from DSWHTKPRAPCPA to DSWPKKKRVPCPA which contains an NLS. The *atfs-1* transcriptional reporter plasmid was generated by PCR amplifying from genomic DNA the 2.4 kb sequence immediately upstream of the *atfs-1* open reading frame and cloned into pPD95.75 using the *SalI* and *BamHI* restriction sites up-stream of the *gfp* open reading frame. All plasmids were confirmed by sequencing. The ATFS-1-expressing transgenic lines were generated by co-injecting the described plasmid (25 ng/μl) with a marker plasmid expressing *myo-3$_{pr}$::mCherry* (60 ng/μl) along with pBluescript (65 ng/μl) into N2 or *atfs-1(tm4525); hsp-60$_{pr}$::gfp* worms generating multiple stable extra-chromosomal arrays.

Cell culture

HeLa cells were transfected with 4μg of GFP or ATFS-1$^{1\text{-}100}$::GFP expressing plasmid via Lipofectamine. The cells were imaged or harvested six hours later and the cells were fractionated as previously described (*5*). It should be noted that ATFS-1$^{1\text{-}100}$::GFP is toxic when expressed in HeLa cells. While mitochondrial localization was observed 4-10 hours following transfection, the cells began dying 12-15 hours post-transfection.

Microscopy

HeLa cells were grown on glass cover slips and imaged on a confocal Nikon Eclipse Ti six hours after transfection. Mitotracker (Invitrogen) was added 30 minutes prior to imaging (*5*). *C. elegans* were imaged using a Zeiss AxioCam MRm mounted on a Zeiss Imager.Z2 microscope.

All comparable *hsp-60$_{pr}$::gfp* images were obtained using the same exposure time except for Figure 3A. The *cco-1*(RNAi) and paraquat images were exposed longer due to worm size and toxicity of the stressors.

Protein analysis and antibodies

Whole worm lysates as well as cellular fractionation were performed as previously described (*5*). Synchronized worms were raised in liquid or on plates under the described conditions to the L4 stage prior to purification via sucrose flotation and cellular fractionation. In Figure 2B, the control worms reached the L4 stage within 50 hours and were harvested and fractionated, however because 100 μg/ml ethidium bromide and *spg-7*(RNAi) impair development, these animals were harvested after five days once they reached the L4 developmental stage and fractionated.

Polyclonal antibodies were generated to amino acids 138-237 of ATFS-1 and subsequently affinity purified by Strategic Diagnostics Inc. Antibodies against α-tubulin were purchased from Calbiochem, NDUFS3 antibodies from MitoSciences and HSP60 from Abcam. Anti-HDEL and GFP antibodies were used as described (*10*). Immunoblots were visualized using an Odyssey Infrared Imager (Li-Cor Biosciences). All western blot experiments were performed multiple times.

Mitochondrial protein import assay

Because steady-state detection of unprocessed MTS containing proteins is very difficult (*12*), we expressed GFP^{mt} and ATFS-1 via the inducible *hsp-16* promoter so that the worms could be harvested and fractionated while either ATFS-1 or GFP^{mt} was actively being translated and imported into mitochondria. *hsp-16$_{pr}$::gfp^{mt}* or *hsp-16$_{pr}$::atfs-1^{FL}* expressing worms were synchronized by bleaching and raised at 16°C in liquid media in the absence or presence of 30 μg/ml ethidium bromide. *hsp-16$_{pr}$::gfp^{mt}* worms were raised on control(RNAi) while *hsp-16$_{pr}$::atfs-1^{FL}* worms were raised on *lon*(RNAi) in order to stabilize ATFS-1^{FL} following mitochondrial import. At the L4 stage (~55 hours following hatching) the worms were shifted to 27°C for one hour to induce expression of either *hsp-16$_{pr}$::gfp^{mt}* or *hsp-16$_{pr}$::atfs-1^{FL}*. Then the worms were harvested by sucrose flotation and fractionated into total, postmitochondrial supernatant and mitochondrial pellet.

RNA isolation and microarray analysis

Total RNA was isolated using the RNA STAT reagent (Tel-Test Inc). RNA samples were prepared from wild-type and *atfs-1(tm4525)* worms fed either control(RNAi) or *spg-7*(RNAi). Worms were synchronized by bleaching and raised in liquid culture under the described conditions and harvested at the L4 stage.

Double-stranded cDNA was synthesized from total RNA using the Affymetrix GeneChip cDNA synthesis kit according to the manufacturer. cDNA was then subjected to in vitro transcription, using the GeneChip IVT Labeling Kit. A measured aliquot of the

biotinylated cRNA product was fragmented and hybridized along with the hybridization control kit onto the GeneChip *C. elegans* genome array (Affymetrix), with incubation for 16 hours at 45˚C and shaking at 60 rev. min^{-1}. The hybridized biotinylated cRNA was stained with streptavidin-phycoerythrin (PE), and then scanned with a GeneChip Array Scanner (Affymetrix). The fluorescence intensity of each probe was quantified using GeneChip Operating Software and GeneChip Analysis Suite (Affymetrix). Data normalization, scaling and 2-way Anova was used to identify differentially expressed genes, using Partek Genomics Suite (v6.5). Average linkage gene clustering was performed with a Euclidean distance using Hierarchical clustering. The genes with statistically significant changes between the treatments and strains were identified using Anova streamlined (Partek Genomic Suite (v6.5)). Only genes with a fold change higher than 1.3 and p-value lower than 0.05 were considered. Genes whose up-regulation in the *atfs-1(tm4525)* background was 25 percent of the up-regulation in wild-type worms were considered ATFS-1 dependent.

Quantitative RT-PCR

Worms were raised and total RNA was isolated as described for the microarray studies. cDNA was then synthesized from total RNA using the iScript™ cDNA Synthesis Kit (Bio-Rad Laboratories). qRT-PCR was used to confirm the expression levels of *atfs-1*, *gfp/gfp^{mt}, lon*, hsp-*60, tim-23, tim-17, gpd-2, skn-1,* and *dnj-10* using iQ™ sybr green supermix and MyiQ™2 Two-Color Real-Time PCR Detection System (Bio-Rad). Gene specific primers are listed in Table S1. Actin was used as a control. Fold changes in gene expression were calculated using the comparative CtΔΔCt method.

Oxygen consumption

Oxygen consumption assays were performed as described (*5*) using a Clark type electrode (*17*).

Fig. S1.

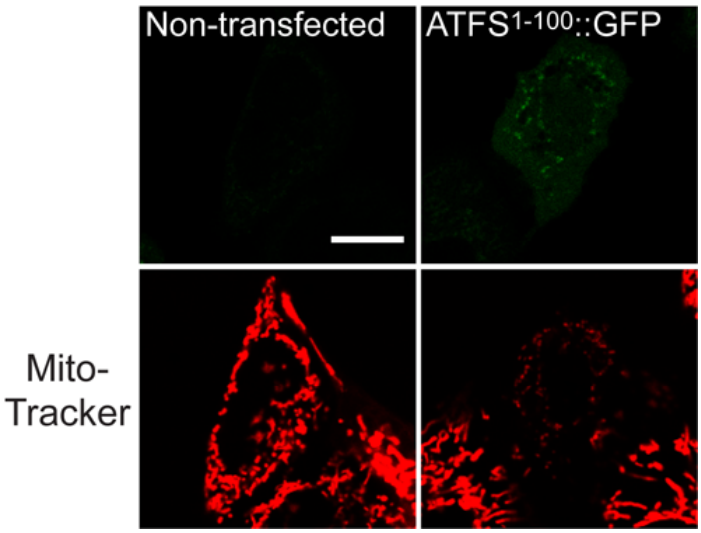

Fig. S1. ATFS-1^{1-100}::GFP localizes to mitochondria and disrupts mitochondrial morphology resulting in death fifteen hours following transfection.
Expression of ATFS-1^{1-100}::GFP caused severe alterations in mitochondrial morphology and cell death ~15 hours post-transfection indicating the fusion protein was toxic. Non-transfected (left panels) or HeLa cells transfected with ATFS-1^{1-100}::GFP (right panels) stained with MitoTracker (lower panels). The displayed cells were imaged fifteen hours following transfection. Because of the defects to mitochondrial morphology and cell death caused by ATFS-1^{1-100}::GFP expression fifteen hours post-transfection, the images and fractionation in Figures 1B & 1C were performed six hours following transfection when the cells appeared healthy. Scale bar, 0.25 mm.

Fig. S2

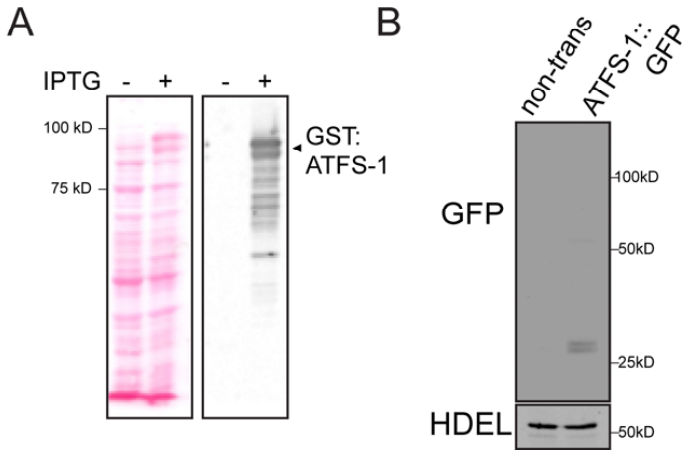
A
IPTG - + - +
100 kD
75 kD
GST:
ATFS-1
B
non-trans
ATFS-1::
GFP
GFP
HDEL
100kD
50kD
25kD
50kD

Fig. S2. Only GFP accumulates in un-stressed *atfs-1$_{pr}$::atfs-1::gfp* transgenic worms. **A.** Ponceau staining and immunoblot of bacterial lysates from control and GST::ATFS-1 expressing cells indicating that the polyclonal ATFS-1 antibodies recognize recombinant ATFS-1. GST::ATFS-1 was induced by incubation with IPTG. **B.** Immunoblots of whole worm extracts from non-transgenic and *atfs-1$_{pr}$::atfs-1::gfp* worms raised on control(RNAi) probed with GFP-specific, or HDEL-specific antibodies as a loading control. Full-length ATFS-1::GFP is predicted to be 90 kDa and was undetectable. However, we observed a 25 kDa band recognized by GFP-specific antibodies suggesting the ATFS-1 portion of the protein is susceptible to degradation.

Fig. S3

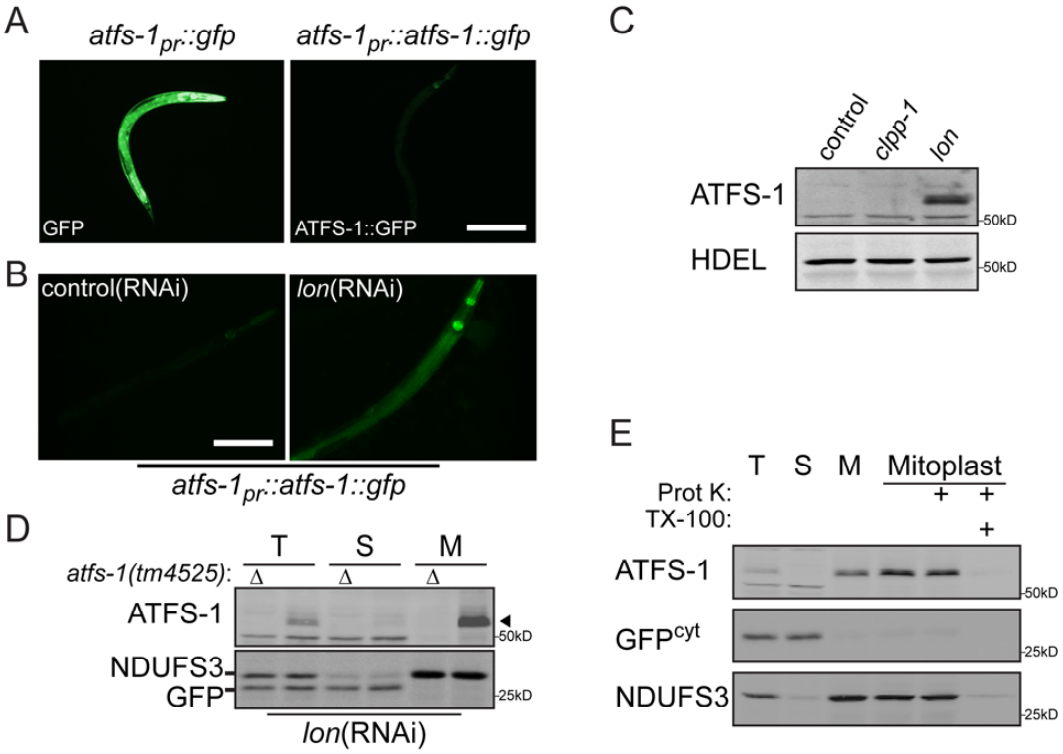
A
atfs-1pr::gfp
atfs-1pr::atfs-1::gfp
GFP
ATFS-1::GFP
B
control(RNAi)
lon(RNAi)
atfs-1pr::atfs-1::gfp
C
control
clpp-1
lon
ATFS-1
HDEL
50kD
50kD
D
T S M
atfs-1(tm4525): Δ Δ Δ
ATFS-1
NDUFS3
GFP
50kD
25kD
lon(RNAi)
E
T S M Mitoplast
Prot K: + +
TX-100: +
ATFS-1
GFPcyt
NDUFS3
50kD
25kD
25kD

Fig. S3. ATFS-1 is degraded within mitochondria by the Lon protease in the absence of UPR^{mt} activation. A. Photomicrographs comparing *atfs-1$_{pr}$::gfp* and *atfs-1$_{pr}$::atfs-1::gfp* expression levels. The *atfs-1* promoter was active as indicated by the accumulation of GFP (left panel), however the weak accumulation of the ATFS-1::GFP (right panel) suggested instability of the fusion protein. Scale bar, 0.25 mm. **B.** Photomicrographs of *atfs-1$_{pr}$::atfs-1::gfp* transgenic worms raised on control or *lon*(RNAi) suggesting the Lon protease degrades ATFS-1::GFP within mitochondria. Scale bar, 0.25 mm. **C.** Immunoblots of extracts from worms raised on control, *clpp-1* or *lon*(RNAi) probed with ATFS-1-specific antibodies or HDEL-specific antibodies as a loading control. **D.** Immunoblots of extracts from *hsp-60$_{pr}$::gfp* wild-type or *atfs-1(tm4525)* (Δ) transgenic worms raised on control or *lon*(RNAi) following cellular fractionation into total lysate (T), postmitochondrial supernatant (S) and mitochondrial pellet (M). The panels were probed with ATFS-1-specific antibodies as well as NDUFS3-specific antibodies (an endogenous mitochondrial protein) and GFP-specific antibody (cytosolic localization). **E.** Immunoblots of extracts from *hsp-60$_{pr}$::gfp* transgenic worms raised on *lon*(RNAi) following cellular fractionation into total lysate (T), postmitochondrial supernatant (S) and mitochondrial pellet (M). Lanes 4-6 are from mitochondria treated with hypotonic buffer to generate mitoplasts and further treated with Triton-X (TX-100) and Proteinase K where indicated. Sub-mitochondrial fractionation was performed as described (*5*). GFP is a cytosolic control and NDUFS3 is a known mitochondrial matrix-localized protein. These data suggest that ATFS-1 accumulates within the mitochondrial matrix when the worms are raised on *lon*(RNAi), which is consistent with Lon being localized to the matrix. However, it should be noted that we were unable to probe the blots for a soluble matrix protein as a control because of the lack of available reagents in *C. elegans*.

Fig. S4

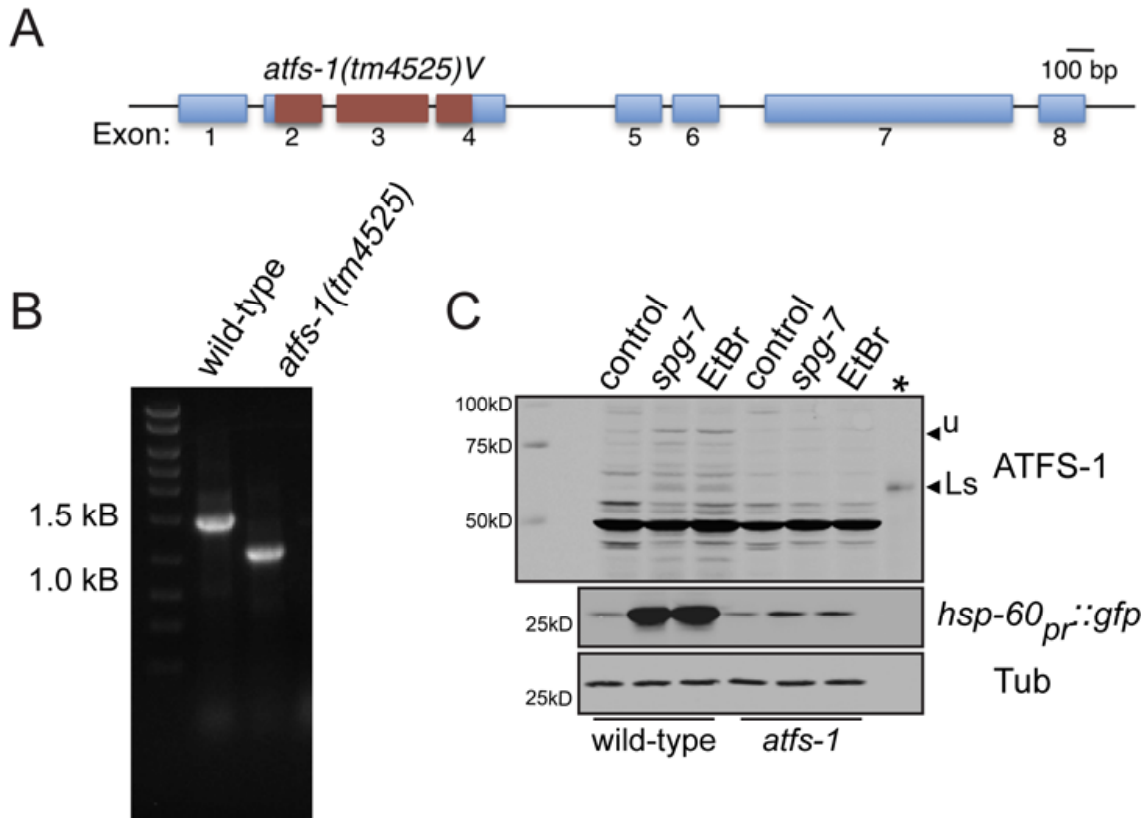
A
atfs-1(tm4525)V
100 bp
Exon: 1 2 3 4 5 6 7 8
B
wild-type
atfs-1(tm4525)
1.5 kB
1.0 kB
C
control
spg-7
EtBr
control
spg-7
EtBr
*
100kD
75kD
50kD
u
Ls
ATFS-1
25kD
hsp-60pr::gfp
25kD
Tub
wild-type
atfs-1

Fig. S4. *atfs-1(tm4525)* worms are unable to induce the UPR^{mt}. A. The *atfs-1(tm4525)* allele lacks 432 base pairs which removes the majority of exons 2 and 4 and all of exon 3. **B.** Ethidium bromide stained PCR products from cDNA generated from wild-type and *atfs-1(tm4525)* worms. Sequence analysis revealed that the expressed *atfs-1(tm4525)* transcript lacked 327 bases. **C.** Immunoblots of lysates from wild-type or *atfs-1(tm4525); hsp-60$_{pr}$::gfp* transgenic worms raised on control, EtBr (100 μg/ml) or *spg-7*(RNAi). The last lane is 3 μg of protein from the mitochondrial pellet of worms raised on *lon*(RNAi). The other lanes are 100 μg of total cell lysate. Unprocessed and *lon*(RNAi)-stabilized (Ls) ATFS-1 are indicated.

Fig. S5

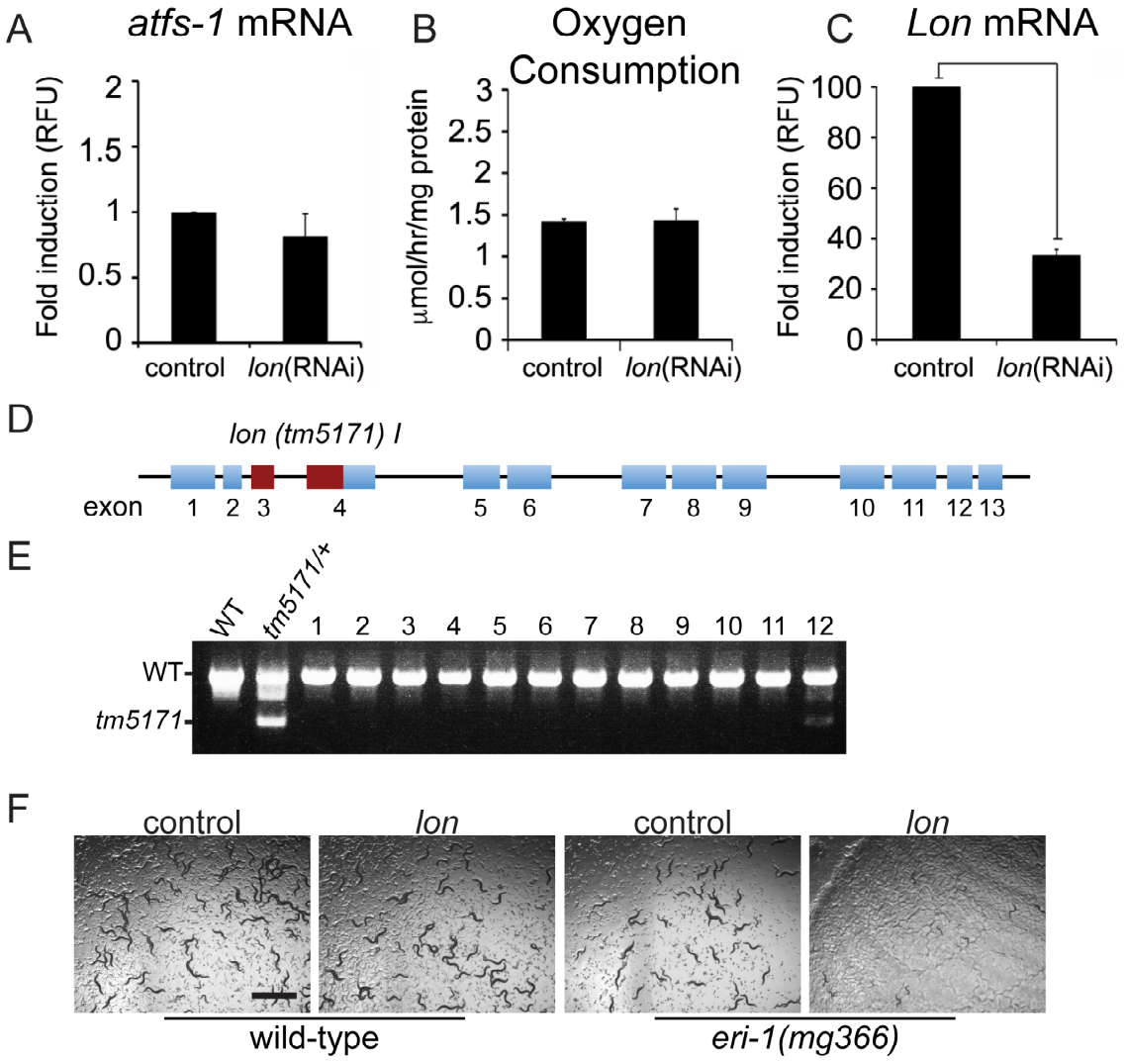
A
atfs-1 mRNA
Fold induction (RFU)
2
1.5
1
0.5
0
control
lon(RNAi)
B
Oxygen Consumption
µmol/hr/mg protein
3
2.5
2
1.5
1
0.5
0
control
lon(RNAi)
C
Lon mRNA
Fold induction (RFU)
100
80
60
40
20
0
control
lon(RNAi)
D
lon (tm5171) I
exon 1 2 3 4 5 6 7 8 9 10 11 12 13
E
WT
tm5171/+
1 2 3 4 5 6 7 8 9 10 11 12
WT
tm5171
F
control
lon
control
lon
wild-type
eri-1(mg366)

Fig. S5. *lon*(RNAi) results in a 70 percent knockdown of *Lon* mRNA, slows ATFS-1 degradation, but does not affect mitochondrial function.
A. Expression levels of *atfs-1* mRNA in wild-type worms raised on control or *lon*(RNAi) determined by qRT-PCR (N = 3, ± SD, p* (student t-test) < 0.05). **B.** Oxygen consumption in synchronized wild-type *hsp-60$_{pr}$::gfp* worms raised on either control or *lon*(RNAi) at the L4 stage. Shown is the mean ± SEM oxygen consumption normalized to protein content (N = 3). These data suggest that *lon*(RNAi) does not significantly affect mitochondrial function. **C.** Expression levels of *lon* mRNA in wild-type worms raised on control or *lon*(RNAi) were determined by qRT-PCR (N = 3, ± SD, p* (student t-test) < 0.05). *lon*(RNAi) caused a 70% reduction in *Lon* mRNA levels. **D.** Schematic of the *Lon* gene, also known as *c34b2.6*, with the *tm5171* deletion highlighted. *tm5171* is a 490 base pair deletion that removes all of exon 3 and a portion of exon 4. **E.** Single worm genotyping (lanes 1-12) of the offspring of a *lon(tm5171)* heterozygote (lane 2). We were unable to identify viable offspring that were homozygous for the *tm5171* deletion suggesting *lon(tm5171)* homozygous worms are inviable. **F.** Photomicrographs comparing growth rates of wild-type and *eri-1(mg366)* raised on control and *lon*(RNAi). Scale bar, 1 mm. The *eri-1(mg366)* allele causes a defect in the RNAi machinery resulting in enhanced RNAi and stronger phenotypes (*18*). Wild-type worms develop normally on *lon*(RNAi) while the majority of the *eri-1(mg366)* worms arrest at the L2 or L3 stage of development. The inviability of the *lon*-deletion worms and severe growth defects of *eri-1(mg366)* worms raised on *lon*(RNAi) suggests that Lon performs essential functions in *C. elegans* similar to those described in other organisms (*19*). However, at 70% *Lon* mRNA knockdown, worm development and mitochondrial function is similar to wild-type worms. These data support the conclusion that in the absence of UPR^{mt} activation, ATFS-1 is imported into mitochondria and degraded by Lon.

Fig. S6

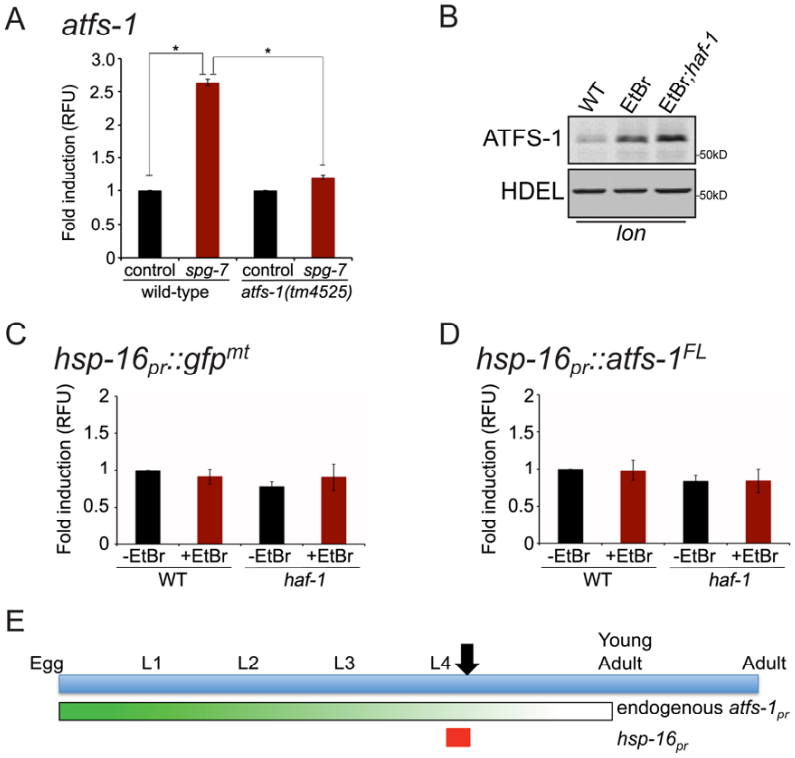
A
atfs-1
Fold induction (RFU)
3.0
2.5
2
1.5
1
0.5
0
control spg-7 control spg-7
wild-type atfs-1(tm4525)
B
WT
EtBr
EtBr;haf-1
ATFS-1
HDEL
50kD
50kD
lon
C
hsp-16pr::gfpmt
Fold induction (RFU)
2
1.5
1
0.5
0
-EtBr +EtBr -EtBr +EtBr
WT haf-1
D
hsp-16pr::atfs-1FL
Fold induction (RFU)
2
1.5
1
0.5
0
-EtBr +EtBr -EtBr +EtBr
WT haf-1
E
Egg
L1
L2
L3
L4
Young Adult
Adult
endogenous atfs-1pr
hsp-16pr

Fig. S6. Endogenous *atfs-1* transcription is induced by mitochondrial stress, however accumulation of *hsp-16$_{pr}$::ATFS-1^{FL}* protein is not due to differences in transcription between wild-type and *haf-1(ok705)* strains. A. Expression levels of *atfs-1* mRNA in wild-type or *atfs-1(tm4525)* worms raised on control or *spg-7*(RNAi) determined by qRT-PCR (N = 3, ± SD, p* (student t-test) < 0.05) indicating that *atfs-1* transcripts are induced during mitochondrial stress probably in a feed-forward manner. **B.** Immunoblots of wild-type and *haf-1(ok705)* worms raised in the absence or presence of 30 μg/ml EtBr on *lon*(RNAi) indicating that more ATFS-1 accumulated within mitochondria during stress in the absence of *haf-1*. This is consistent with HAF-1 being a negative regulator of mitochondrial protein import. However, we were unable to detect the uncleaved cytosolic form of ATFS-1 during these relatively mild stress conditions when HAF-1 was required for UPR^{mt} induction (Fig. 3B). Therefore, we examined ATFS-1, expressed via the *hsp-16* promoter which allows higher expression levels (Fig. 2D). **C.** Expression levels of *gfp^{mt}* mRNA via the *hsp-16* promoter in wild-type or *haf-1(ok705)* worms raised in the absence or presence of 30 μg/ml ethidium bromide determined by qRT-PCR (N = 3, ± SD, p* (student t-test) < 0.05). A control experiment for Figure 2C indicating the *hsp-16* promoter is unaffected by mitochondrial stress or the *haf-1*-deletion. **D.** Expression levels of *atfs-1^{FL}* mRNA expressed from the *hsp-16* promoter in wild-type or *haf-1(ok705)* worms raised in the absence or presence of 30 μg/ml ethidium bromide determined by qRT-PCR (N = 3, ± SD, p* (student t-test) < 0.05). A control experiment for Figure 2D indicating the *hsp-16* promoter is unaffected by mitochondrial stress or the *haf-1*-deletion. **E.** Schematic indicating when during the *C. elegans* lifecycle endogenous *atfs-1* is expressed and when *hsp-16$_{pr}$::atfs-1^{FL}* was induced to examine mitochondrial import of ATFS-1 (Fig. 2D). The expression of *atfs-1* from the endogenous promoter is strongest early in development when the worms are small and then diminishes over time as they develop (*20, 21*) making it experimentally challenging to examine ATFS-1 localization when ATFS-1 is actively being translated and imported. Therefore, *hsp-16$_{pr}$::atfs-1^{FL}* animals were raised to the L4 stage and then shifted from 16°C to 27°C for one hour (red bar) to induce ATFS-1 expression prior to harvesting when mRNA was purified (fig. S6D) and worms were fractionated (Fig. 2D).

Fig. S7

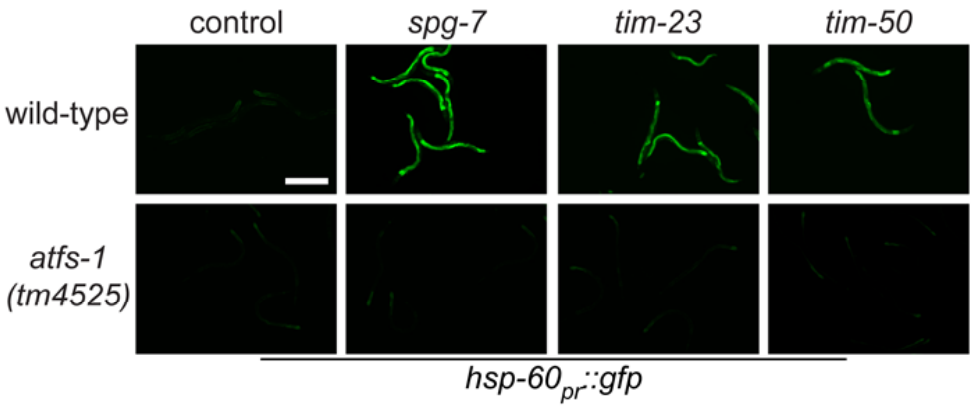
control
spg-7
tim-23
tim-50
wild-type
atfs-1
(tm4525)
hsp-60pr::gfp

Fig. S7. Knockdown of SPG-7 or components of the TIM23 complex activate the UPR^{mt} in an ATFS-1-dependent manner. Fluorescent photomicrographs of wild-type or *atfs-1(tm4525); hsp-60$_{pr}$::gfp* transgenic worms raised on control, *spg-7*, *tim-23* or *tim-50*(RNAi). Scale bar, 0.5 mm.

Fig. S8

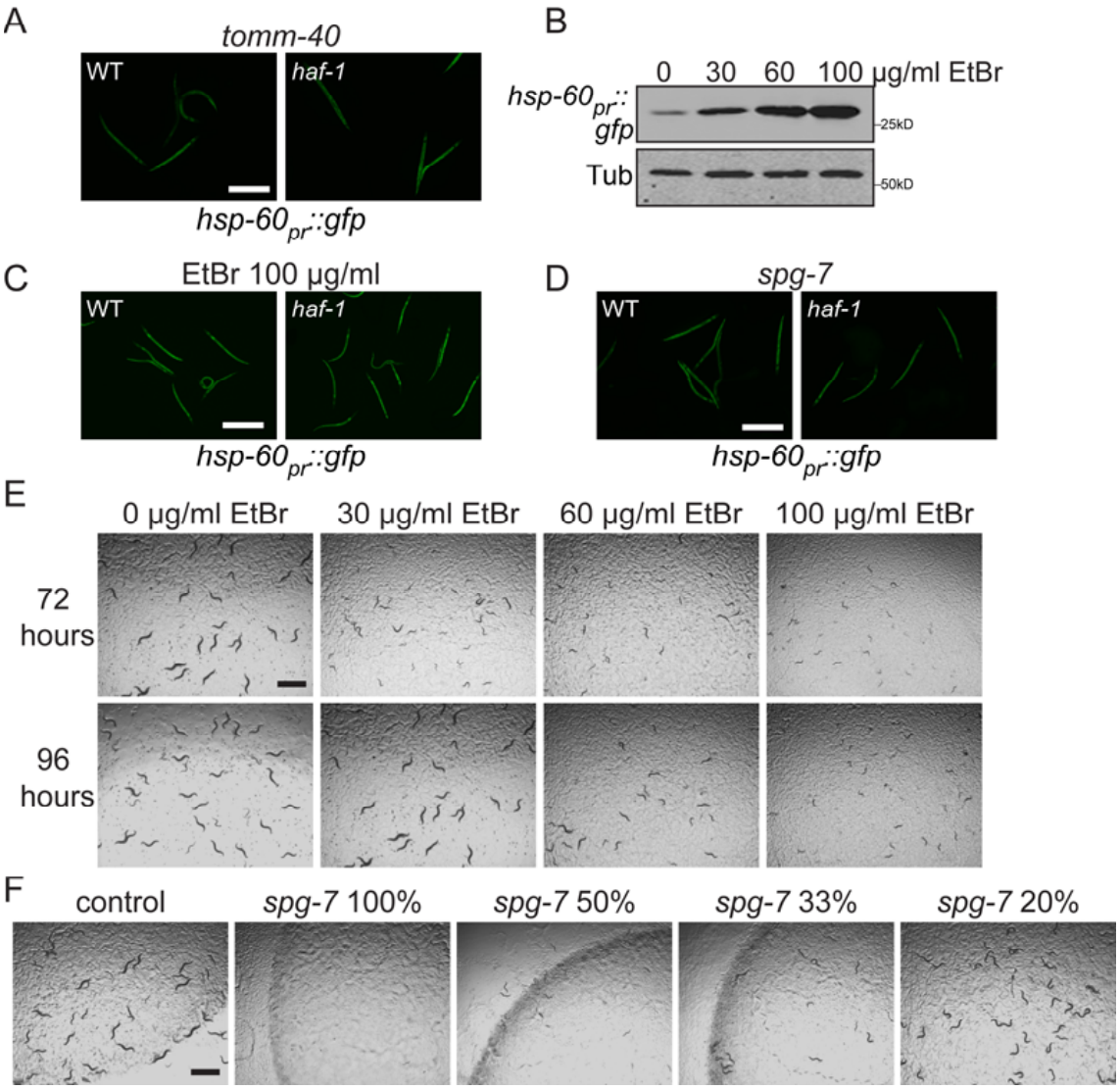
A
tomm-40
WT
haf-1
hsp-60pr::gfp
B
0 30 60 100 µg/ml EtBr
hsp-60pr::gfp
25kD
Tub
50kD
C
EtBr 100 µg/ml
WT
haf-1
hsp-60pr::gfp
D
spg-7
WT
haf-1
hsp-60pr::gfp
E
0 µg/ml EtBr
30 µg/ml EtBr
60 µg/ml EtBr
100 µg/ml EtBr
72 hours
96 hours
F
control
spg-7 100%
spg-7 50%
spg-7 33%
spg-7 20%

Fig. S8. Treatment with high doses of ethidium bromide or *spg-7*(RNAi) caused developmental arrest and UPR^{mt} activation independent of *haf-1*.
A. Photomicrographs of wild-type and *haf-1(ok705); hsp-60$_{pr}$::gfp* raised on control or *tomm-40*(RNA) indicating that direct perturbations to the mitochondrial import channel activate the UPR^{mt} independent of *haf-1*. Scale bar, 0.5 mm. **B.** Immunoblots of *hsp-60$_{pr}$::gfp* worms raised in the presence of 0, 30, 60 or 100 μg/ml EtBr indicating dose responsive UPR^{mt} activation. **C.** Photomicrographs of wild-type and *haf-1(ok705); hsp-60$_{pr}$::gfp* raised on 100 μg/ml EtBr indicating that UPR^{mt} activation during high doses of EtBr does not require *haf-1*. **D.** Photomicrographs of wild-type and *haf-1(ok705); hsp-60$_{pr}$::gfp* raised on control or *spg-7*(RNA). Scale bar, 0.5 mm. **E.** Photomicrographs of wild-type worms synchronized and raised on 0, 30, 60 and 100 μg/ml EtBr and imaged 72 (top panels) and 96 (lower panels) hours later. Scale bar, 1 mm. While the worms on 30 μg/ml EtBr developed somewhat slower than untreated worms, they were able to develop and reproduce. However, worms raised on 100 μg/ml EtBr developmentally arrested and were unable to reproduce. At 30 μg/ml EtBr, *haf-1* is required for *hsp-60$_{pr}$::gfp* induction while at 100 μg/ml EtBr *haf-1* was not required (Figs. 3A & S8C). **F.** Photomicrographs of wild-type worms raised on control or dilutions of *spg-7*(RNAi). Scale bar, 1 mm. L4 worms on undiluted (100%) *spg-7*(RNAi) reproduced poorly and the offspring were unable to develop beyond the L2 stage (second panel). These animals activated *hsp-60$_{pr}$::gfp* expression independent of *haf-1* (fig. S8D). If however, the worms were raised on *spg-7*(RNAi) diluted with an inert RNAi (*gfp*(RNAi)), development is impaired but the worms are able to mature to adults and reproduce (panels 4-5) similar to 30 μg/ml EtBr.

Fig. S9

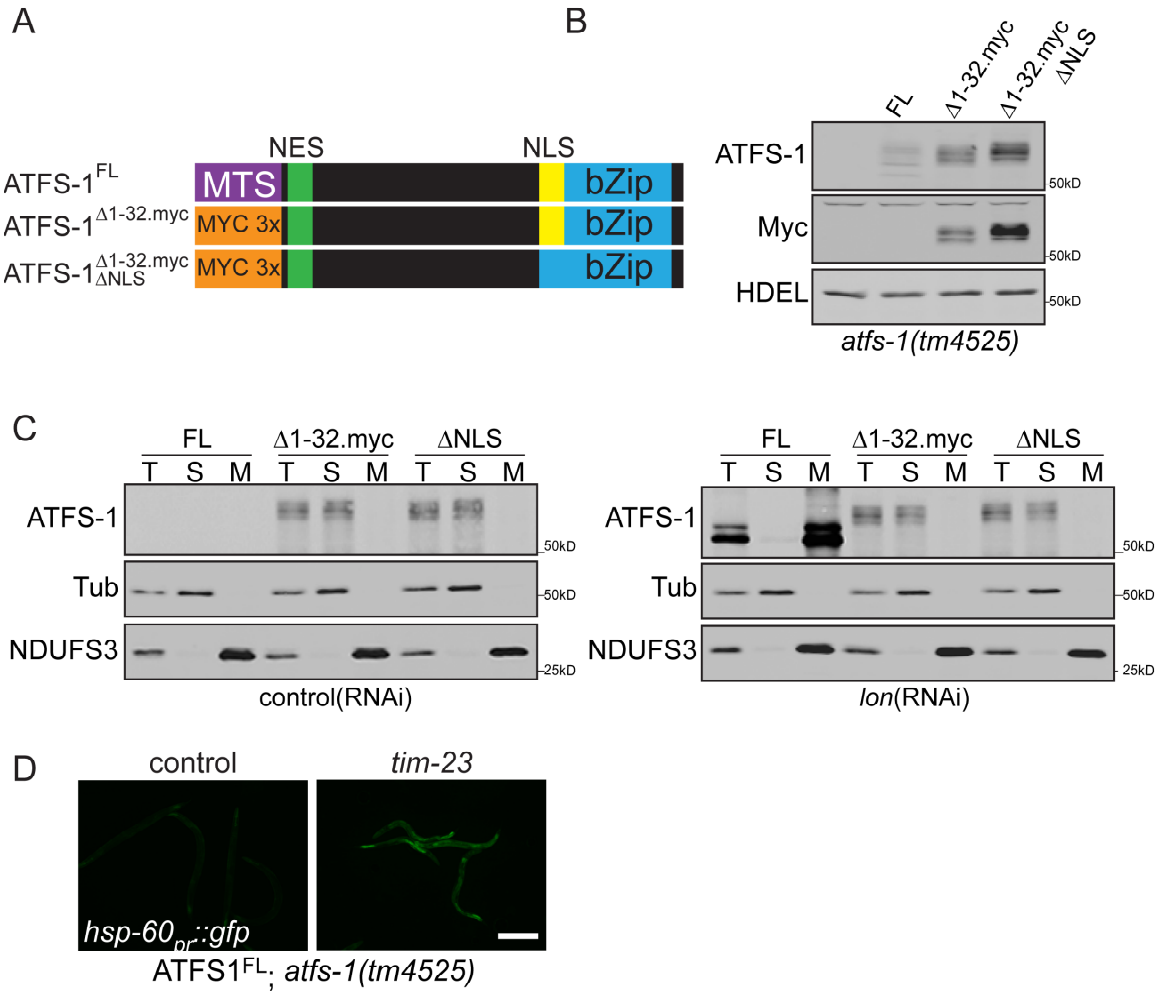
A
NES
NLS
ATFS-1FL
MTS
bZip
ATFS-1Δ1-32.myc
MYC 3x
bZip
ATFS-1Δ1-32.myc ΔNLS
MYC 3x
bZip
B
FL
Δ1-32.myc
Δ1-32.myc ΔNLS
ATFS-1
Myc
HDEL
50kD
50kD
50kD
atfs-1(tm4525)
C
FL
Δ1-32.myc
ΔNLS
T S M T S M T S M
ATFS-1
Tub
NDUFS3
50kD
50kD
25kD
control(RNAi)
lon(RNAi)
D
control
tim-23
hsp-60pr::gfp
ATFS1FL; atfs-1(tm4525)

Fig. S9. Function and cellular localization of transgene-expressed ATFS-1^{FL}, ATFS-1$^{\Delta 1\text{-}32.myc}$ and ATFS-1$^{\Delta 1\text{-}32.myc.\Delta NLS}$. A. Schematic of the transgene-expressed ATFS-1 variants: wild-type or full-length (^{FL}) ATFS-1, ATFS-1 where the amino-terminal 32 amino acids were replaced with three Myc-epitope tags ($^{\Delta 1\text{-}32.myc}$) and ATFS-1$^{\Delta 1\text{-}32.myc}$ lacking the nuclear localization sequence ($^{\Delta 1\text{-}32.myc.\Delta NLS}$). All transgenes were expressed via the *hsp-16* promoter in *atfs-1(tm4525); hsp-60$_{pr}$::gfp* worms. **B.** Immunoblots of whole worm lysates from non-transgenic, ATFS-1^{FL}, ATFS-1$^{\Delta 1\text{-}32.myc}$, and ATFS-1$^{\Delta 1\text{-}32.\Delta NLS}$ worms following incubation at 30°C for 8 hours to induce expression of the ATFS-1 variants. Lysates were prepared immediately following incubation at 30°C. Immunoblots were probed with ATFS-1-specific antibodies that recognized all three ATFS-1 variants (top panel). Anti-myc antibodies recognized the myc-epitope in ATFS-1$^{\Delta 1\text{-}32.myc}$ and ATFS-1$^{\Delta 1\text{-}32.\Delta NLS}$ (middle panel). **C.** Immunoblots of extracts from *hsp-16$_{pr}$::ATFS-1^{FL}*, *hsp-16$_{pr}$::ATFS-1$^{\Delta 1\text{-}32.myc}$* and *hsp-16$_{pr}$::* ATFS-1$^{\Delta 1\text{-}32.\Delta NLS}$ expressing worms raised on control (left panels) or *lon*(RNAi) (right panels) following subcellular fractionation. As expected ATFS-1^{FL} localized to mitochondria, which was only detectable when the worms were raised on *lon*(RNAi). Both ATFS-1$^{\Delta 1\text{-}32.myc}$ and ATFS-1$^{\Delta 1\text{-}32.myc.\Delta NLS}$ were excluded from mitochondria and unaffected by *lon*(RNAi) which is consistent with the nuclear accumulation of ATFS-1$^{\Delta 1\text{-}32.myc}$::GFP (Fig. 2A). Worms were raised to the L4 stage at 16°C and shifted to 30°C for 2 hours. The animals were harvested 9 hours later and fractionated. **D.** Photomicrographs of *hsp-16$_{pr}$::ATFS-1^{FL}* expressing worms raised on control or *tim-23*(RNAi) indicating that ATFS-1^{FL} expressed via the *hsp-16* promoter was capable of activating the UPR^{mt} and thus a functional transgene-expressed protein. Scale bar, 0.5 mm.

Fig. S10

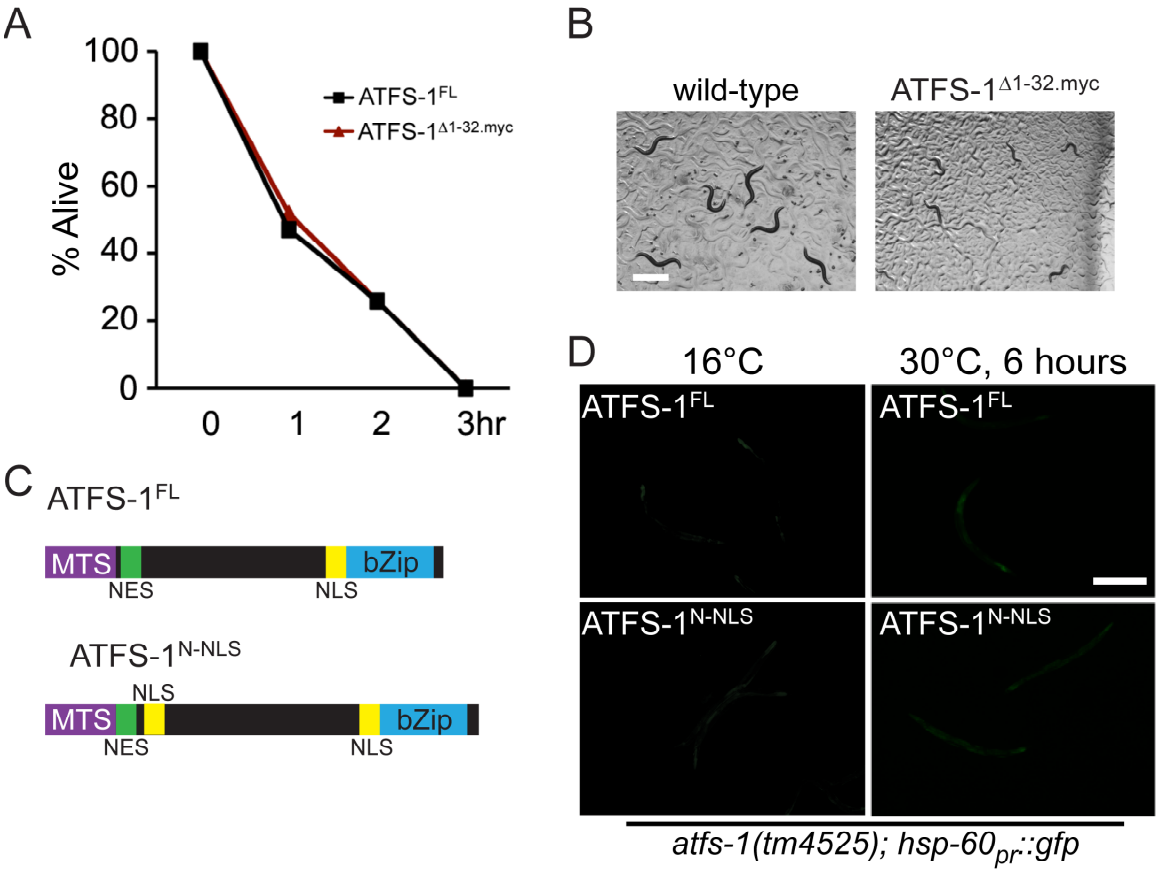
A
100
80
60
40
20
0
% Alive
0
1
2
3hr
ATFS-1FL
ATFS-1Δ1-32.myc
B
wild-type
ATFS-1Δ1-32.myc
C
ATFS-1FL
MTS
bZip
NES
NLS
ATFS-1N-NLS
NLS
MTS
bZip
NES
NLS
D
16°C
30°C, 6 hours
ATFS-1FL
ATFS-1FL
ATFS-1N-NLS
ATFS-1N-NLS
atfs-1(tm4525); hsp-60pr::gfp

Fig. S10. Constitutive activation of the UPR^{mt} by ATFS-1$^{\Delta 1\text{-}32}$ does not confer resistance to mitochondrial stress. A. Survival of L4 wild-type and *hsp-16$_{pr}$::atfs-1$^{\Delta 1\text{-}32.myc}$* worms on 300 mM paraquat indicating that constitutive UPR^{mt} activation by ATFS-1$^{\Delta 1\text{-}32.myc}$ does not confer stress resistance. **B.** Photomicrographs of 3 day old wild-type and *hsp-16$_{pr}$::atfs-1$^{\Delta 1\text{-}32.myc}$* worms indicating that worms expressing ATFS-1$^{\Delta 1\text{-}32.myc}$ develop more slowly than wild-type worms. Scale bar, 1 mm. **C.** Schematic comparing full length ATFS-1 (ATFS-1^{FL}) and ATFS-1 with a NLS inserted near the N-terminus (ATFS-1$^{N\text{-}NLS}$). **D.** Photomicrographs of ATFS-1^{FL} or ATFS-1$^{N\text{-}NLS}$ expressing *atfs-1(tm4525); hsp-60$_{pr}$::gfp* worms raised at 16°C or raised at 16°C and incubated at 30°C for 6 hours to further induce expression of the transgene. At both temperatures, *hsp-60$_{pr}$::gfp* expression was similar indicating that inserting a NLS nearer to the N-terminus had no impact on ATFS-1 regulation. Scale bar, 0.25 mm.

Fig. S11

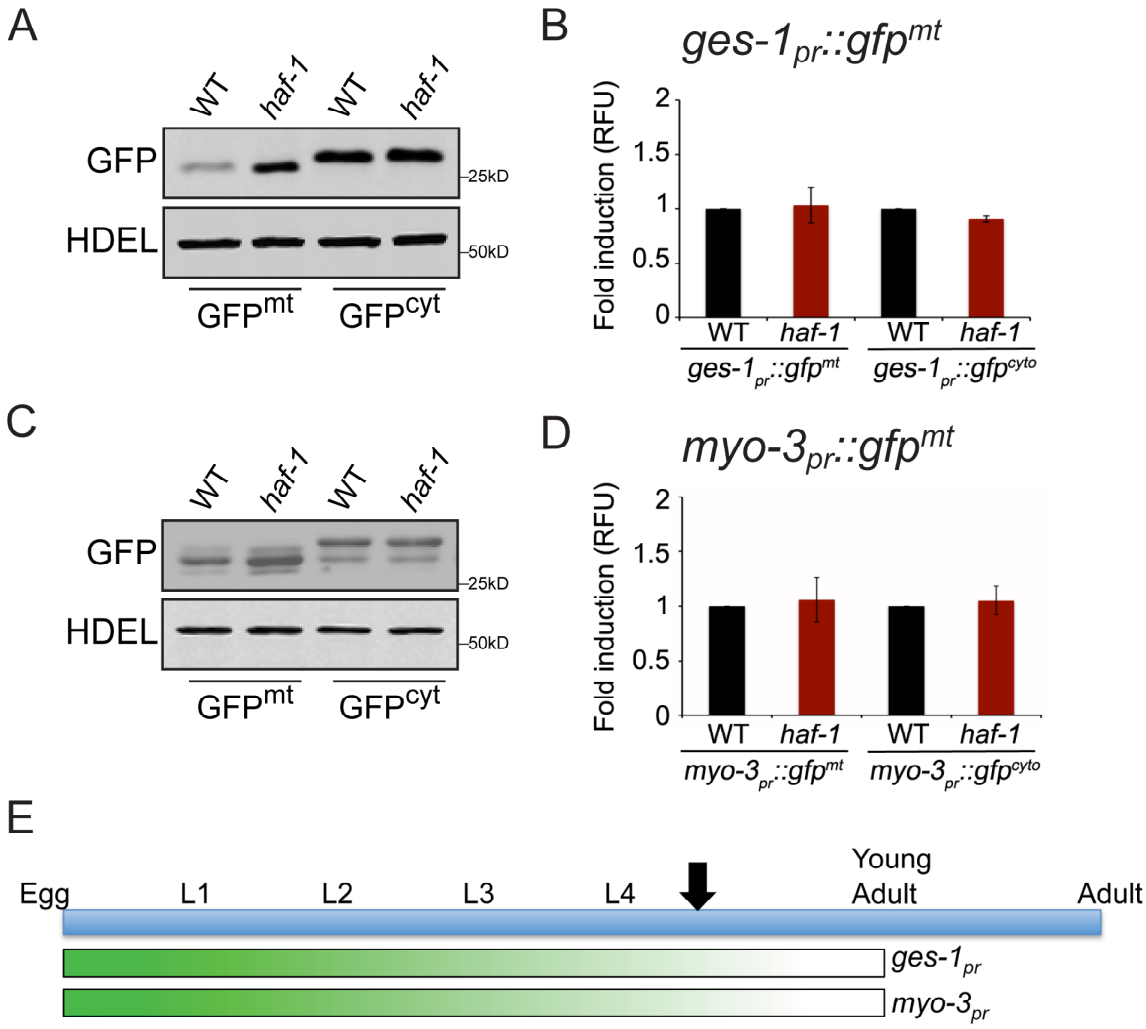
A
WT
haf-1
WT
haf-1
GFP
HDEL
25kD
50kD
GFPmt
GFPcyt
B
ges-1pr::gfpmt
Fold induction (RFU)
2
1.5
1
0.5
0
WT
haf-1
WT
haf-1
ges-1pr::gfpmt
ges-1pr::gfpcyto
C
WT
haf-1
WT
haf-1
GFP
HDEL
25kD
50kD
GFPmt
GFPcyt
D
myo-3pr::gfpmt
Fold induction (RFU)
2
1.5
1
0.5
0
WT
haf-1
WT
haf-1
myo-3pr::gfpmt
myo-3pr::gfpcyto
E
Egg
L1
L2
L3
L4
Young Adult
Adult
ges-1pr
myo-3pr

Fig. S11. More GFP^{mt} accumulates within mitochondria of *haf-1(ok705)* worms compared to wild-type worms. A. Immunoblots of extracts from wild-type or *haf-1(ok705)* worms expressing intestine-specific *ges-1$_{pr}$::GFP^{mt}* or *ges-1$_{pr}$::GFP^{cyt}*. More GFP^{mt} accumulated in worms lacking *haf-1*, however similar amounts of GFP lacking the MTS accumulated in both strains (GFP^{cyt}, lanes 3 & 4), indicating that the increased GFP^{mt} accumulation was dependent on both *haf-1(ok705)* and the MTS. **B.** Expression levels of *ges-1$_{pr}$::gfp^{mt}* or *ges-1$_{pr}$::gfp^{cyt}* mRNA in wild-type or *haf-1(ok705)* worms determined by qRT-PCR (N = 3, ± SD, p* (student t-test) < 0.05). **C.** Immunoblots of extracts from wild-type or *haf-1(ok705)* worms expressing muscle-specific *myo-3$_{pr}$::GFP^{mt}* or *myo-3$_{pr}$::GFP^{cyt}*. More GFP^{mt} accumulated in worms lacking *haf-1*, however similar amounts of GFP lacking the MTS accumulated in both strains (GFP^{cyt}, lanes 3 & 4), indicating that the increased GFP^{mt} accumulation was dependent on both *haf-1(ok705)* and the MTS. **D.** Expression levels of *myo-3$_{pr}$::gfp^{mt}* or *myo-3$_{pr}$::gfp^{cyt}* mRNA in wild-type or *haf-1(ok705)* worms determined by qRT-PCR (N = 3, ± SD, p* (student t-test) < 0.05). **E.** Schematic indicating when during *C. elegans* development expression of *ges-1$_{pr}$::gfp^{mt}* and *myo-3$_{pr}$::gfp^{mt}* occurs and when the worms were harvested for mRNA or protein analysis (black arrow). When expressed via the strong *ges-1* and *myo-3* promoters, GFP^{mt} causes unfolded protein stress and slows development, presumably because of an increase in the import of unfolded GFP^{mt} which challenges the mitochondrial protein folding environment (*10, 22*). Similar to the *atfs-1* promoter, the *ges-1* and *myo-3* promoters are most active early in development and diminish over time. Also similar to ATFS-1 (Fig. 3B), more processed GFP^{mt} accumulated in *haf-1(ok705)* worms relative to wild-type worms. Because expression of *gfp^{mt}* and accumulation of GFP lacking the MTS in the cytosol were unaffected by the *haf-1(ok705)*-deletion, these results suggest that the accumulation of processed GFP^{mt} was due to differences in mitochondrial import efficiency between the wild-type and *haf-1(ok705)* worms.

Fig. S12

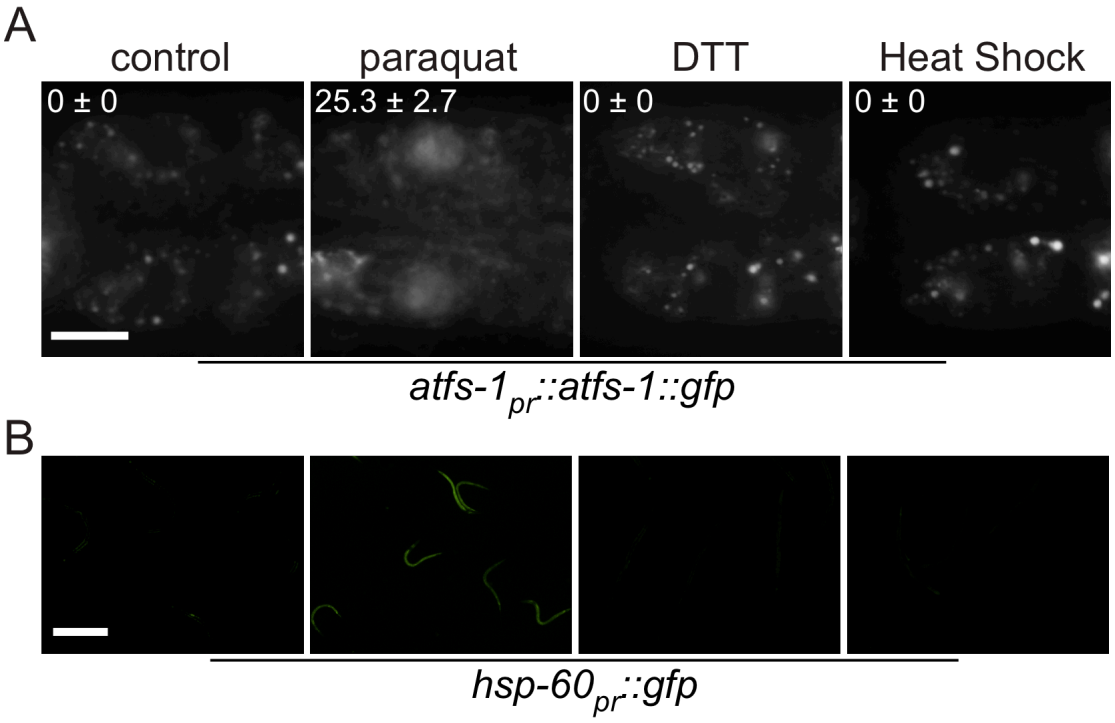
A
control
paraquat
DTT
Heat Shock
0 ± 0
25.3 ± 2.7
0 ± 0
0 ± 0
atfs-1pr::atfs-1::gfp
B
hsp-60pr::gfp

Fig. S12. ATFS-1 nuclear accumulation and UPR^{mt} activation is specific to mitochondrial stress. A. Photomicrographs of the two proximal intestinal cells in *atfs-1$_{pr}$::atfs-1::gfp* transgenic animals raised in the presence of 0.5 mM paraquat, dithiothreitol (5 mM DTT) for 24 hours to cause endoplasmic reticulum stress, or at 30°C for 5 hours to cause heat shock. ATFS-1::GFP only accumulated in the nuclei of worms exposed to paraquat, which activates the UPR^{mt} (Figs. 3A & S12B). The mean percentage ± SEM of worms with nuclear accumulation of ATFS-1::GFP is indicated (N = 3). Scale bar, 15 μm. **B.** Photomicrographs of *hsp-60$_{pr}$::gfp* worms raised in the presence of 0.5 mM paraquat, dithiothreitol (5 mM DTT), or at 30°C. Consistent with ATFS-1::GFP nuclear accumulation (fig. S12A), only paraquat activated *hsp-60$_{pr}$::gfp* expression indicating ATFS-1 and the UPR^{mt} are activated specifically by mitochondrial stress. Scale bar, 0.5 mm.

Fig. S13

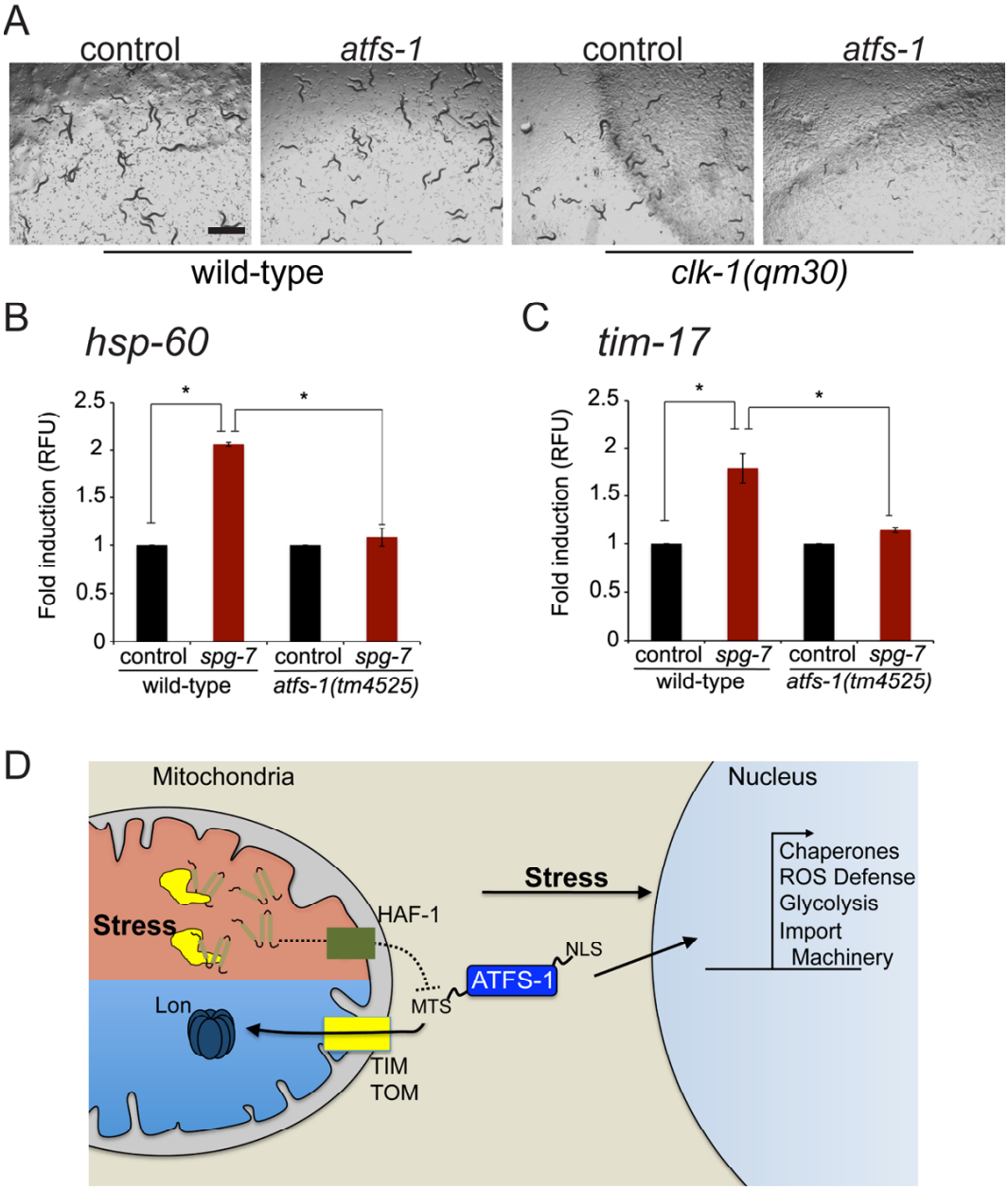
A
control
atfs-1
control
atfs-1
wild-type
clk-1(qm30)
B
hsp-60
Fold induction (RFU)
2.5
2
1.5
1
0.5
0
*
*
control
spg-7
control
spg-7
wild-type
atfs-1(tm4525)
C
tim-17
Fold induction (RFU)
2.5
2
1.5
1
0.5
0
*
*
control
spg-7
control
spg-7
wild-type
atfs-1(tm4525)
D
Mitochondria
Nucleus
Stress
HAF-1
Stress
NLS
ATFS-1
MTS
Lon
TIM
TOM
Chaperones
ROS Defense
Glycolysis
Import
Machinery

Fig. S13. During mitochondrial stress, ATFS-1 is required for development and the induction of *hsp-60* as well as TIM23 complex components. A. Representative photomicrographs of wild-type or *clk-1(qm30)* worms raised on control or *atfs-1*(RNAi). Scale bar, 1 mm. **B-C.** Expression levels of *hsp-60* and *tim-17* mRNA in wild-type or *atfs-1(tm4525)* worms raised on either control or *spg-7*(RNAi) worms determined by qRT-PCR (N = 3, ± SD, p* (student t-test) < 0.05). **D.** In the absence of mitochondrial stress, ATFS-1 is efficiently imported into mitochondria and degraded by the Lon protease as a means of repressing UPR^{mt} signaling (blue). In the presence of mitochondrial dysfunction or unfolded protein stress in the mitochondrial matrix (red), import efficiency is reduced causing a percentage of ATFS-1 to accumulate in the cytosol. Because ATFS-1 has an NLS, it then traffics to the nucleus where it mediates the transcriptional induction of many genes to promote mitochondrial protein folding and protect against the consequences of dysfunctional mitochondria. If the mitochondrial defect is due to perturbations that directly impair import such as the mitochondrial protein import channels (TIM23) or the electron transport chain, this is sufficient to slow protein import allowing ATFS-1 to traffic to the nucleus. However, if the stress is due to unfolded proteins within the matrix, HAF-1, is required to slow import allowing ATFS-1 to traffic to the nucleus.

Table S1. Sequences of primers used in quantitative real time-PCR reactions.

Gene	Primer Sequence
act-3	F: 5'-ATCCGTAAGGACTTGTACGCCAAC-3' R: 5'-CGATGATCTTGATCTTCATGGTTC-3'
hsp-60	F: 5'-AGGGATTCGAGAGCATTCGTCAAG-3' R: 5'-TGTGGCGACTTGAGCGATCTCTTC-3'
tim-23	F: 5'-CAACTGAAATCTGCTGGAGTAGGAG-3' R: 5'-GGCATAATGTATTGCGGCTGC-3'
drp-1	F: 5'-TGGATTCCTTGGATTATTCGGC-3' R: 5'-AGTTGCGTCTCTGGCACTTCTG-3'
dnj-10	F: 5'-GCGGGCTCATTCATCGATCTGTAC-3' R: 5'-CAGATTTTTTGTCGACACCCAAAG-3'
gpd-2	F: 5'-TGAAATCCAATGGGGAGCCTC-3' R: 5'-GGAGCAGAGATGATGACCTTCTTG-3'
skn-1	F: 5'-TCCACCAGCATCTCCATTCG-3' R: 5'-CTCCATAGCACATCAATCAAGTCG-3'
tim-17	F: 5'-GATTGTTGTCTTGTCGCCATCC-3' R: 5'-ATCACCTTTGGTCCTGAACGG-3'
atfs-1	F: 5'-CAATCACCATCAAAATCGGCG-3' R: 5'-CTTGCTCAATGTCCATTTCGAAC 3'
gfp	F: 5'-CATGGCAGACAAACAAAAGAATG 3' R: 5'-CTGCTAGTTGAACGCTTCCATC 3'
lon	F: 5'-CGAAGGCTACGATGATGGC 3' R: 5'-GAAGTAGAAGATTGATTTGTTGACCG 3'

Additional Data (separate files)

Table S2. Genes up-regulated during *spg-7*(RNAi) treatment. Genes whose expression was differentially increased in worms raised on *spg-7*(RNAi) compared to those raised on control(RNAi).

Table S3. Genes up-regulated during *spg-7*(RNAi) treatment dependent on *atfs-1*. Genes whose expression was differentially decreased in *atfs-1(tm4525)* relative to wild-type worms both raised on *spg-7*(RNAi).